TOP-SANDIA

Sandia National Laboratories

Albuquerque, New Mexico 87185

date: February 29, 1984

to: J. L. Telford and S. B. Burson

M Berman Randall K Cole, Jr.

from: M. Berman and R. K. Cole, Jr., 6427

subject: Status of Core Melt Programs -- November-December 1983

I. Core Melt - Coolant Interactions

1.0 Presentations and Meetings

A. J. Wickett presented a paper at the 1983 ANS Winter Meeting in San Francisco, CA, October 30-November 3, entitled "Monte Carlo Analysis of Steam Explosions Revisited," by M. Berman, D. V. Swenson, and A. J. Wickett. M. L. Corradini and M. Berman attended the Containment Loads Working Group Meeting on November 17-18, at Argonne National Laboratory. Corradini made several presentations.

The IDCOR accident phenomenology reports were independently reviewed by M. Berman and A. J. Wickett, K. Bergeron, et al. Several presentations were made at the NRC-IDCOR Meeting in Harper's Ferry, WV, on November 29-December 1. M. Berman presented a paper which reviewed the IDCOR report 14.1 A: "Key Phenomenological Models for Assessing Explosive Steam Generation Rates." M. Berman and K. Bergeron made presentations reviewing the IDCOR report on nonexplosive steam generation, and also presented some recent FCI experimental results. M. Berman gave the summary presentation on steam explosions.

On December 12, M. Berman made a three-hour presentation reviewing the FCI program and status to D. F. Ross and R. M. Bernero of the NRC. Bill Bohl and Skip Dearien of LASL met with Bob Wright (NRC), Bill Camp, and M. Berman on December 13 to discuss LASL contributions to resolving important FCI questions. The group agreed that focusing computational efforts on the behavior of the in-vessel water "slug" would not be fruitful. LASL will continue to explore the development of computational models to assist in understanding and predicting FCI phenomena. On December 14, M. Berman gave an invited seminar on "Core Melt - Coolant Interactions" to the Electric Power Research Institute in Palo Alto, CA.

2.0 Intermediate Scale Experiments
(M. S. Krein, M. Berman)

2.1 Introduction

The major activities of this reporting period included the refurbishment of the FITS chamber, in preparation for the D series of experiments, and the performance of test FITS1D. A great deal of effort was required in the initial chamber set-up for the FITSD series of tests. This was due to the fact that the Hydrogen program had been using the facility for more than a year since the last in-chamber steam explosion series had been run. A general reconfiguration of the entire control and instrumentation equipment was also accomplished during this reporting period. Several additions to the on-site data reduction capabilities were made in conjunction with the chamber set-up, control, and instrumentation equipment overhaul.

The original FITSD series test plan has been under review by the NRC and may be changed before the performance of the second experiment of the series.

A brief description of the initial conditions and the results of test 1D are given below.

2.2 FITS1D

The primary objective of the FITSD series of experiments, outlined under the original test plan, were to begin an investigation of those characteristics of an FCI which have been proposed to lead to indirect containment failure. These characteristics include steam generation, hydrogen generation, and direct containment heating for explosive as well as nonexplosive fuel-coolant interactions. The nature of the resultant debris is also of interest.

Only one experiment was performed. No further D-series experiments are planned until the revised test plan is returned from the NRC.

2.2.1 Initial Conditions

The FITS1D experiment utilized 20 kg of an Fe_3O_4/Al thermite delivered into a 61 cm square lucite water chamber. The water was 61 cm deep and was near the saturation temperature. The FITS chamber atmosphere had been purged twice and inerted with N_2 at atmospheric pressure. Melt hold time was 1.5 seconds and the drop height was 1.82 m. An aluminum foil cover was placed over the water chamber to prevent condensation on the camera ports.

2.2.2 Instrumentation

A major objective of the test was met: checkout of instrumentation which detected and recorded chamber pressurization as a function of time, chamber temperature as a function of time, and volumetric hydrogen generation averaged over 1-minute intervals. Chamber pressurization was detected by thermally protected strain-gage pressure transducers; five transducers were placed in various locations in the FITS chamber head and walls. Two type K thermocouples were used to detect changes in the chamber atmospheric temperature. Volumetric hydrogen generation was determined through analysis of gas samples that were taken during the course of the interaction at intervals of 1 minute.

2.2.3 Results

With the exception of a slow thermite burn, all systems and devices functioned properly. A fairly coherent melt was delivered to the water chamber. Camera data were hampered by port fogging but revealed a nonexplosive event dominated by a vigorous surface expulsion similar to the surface events seen in the CM series of experiments.

No substantial water phase pressure pulses were produced. A plot of chamber pressurization resulting from steam and hydrogen and direct containment heating is shown in Figure 1. This record shows two distinct events which contributed to the ultimate pressurization of the FITS chamber. The first event resulted in the steep pressure rise with a duration of about 0.200 s. Although a thorough analysis of all the data has not yet been completed, some of the initial steep pressure rise for this nonexplosive interaction may be a result of direct chamber heating via the ejection and fragmentation of unquenched melt; a large part of the pressure rise is probably due to surface reactions similar to those observed in the CM-series of tests. The second event, characterized by the much more gradual change in the slope of Figure 1, may indicate a pressure increase dominated by residual steam and hydrogen generation. A peak pressure of about 1.8 bars occurred at about 3 seconds after pressurization began.

A rapid increase in chamber temperature, shown on Figure 2, suggests that both direct heating and the surface expulsion of molten fuel were involved in this FCI. The characteristics of chamber pressurization and

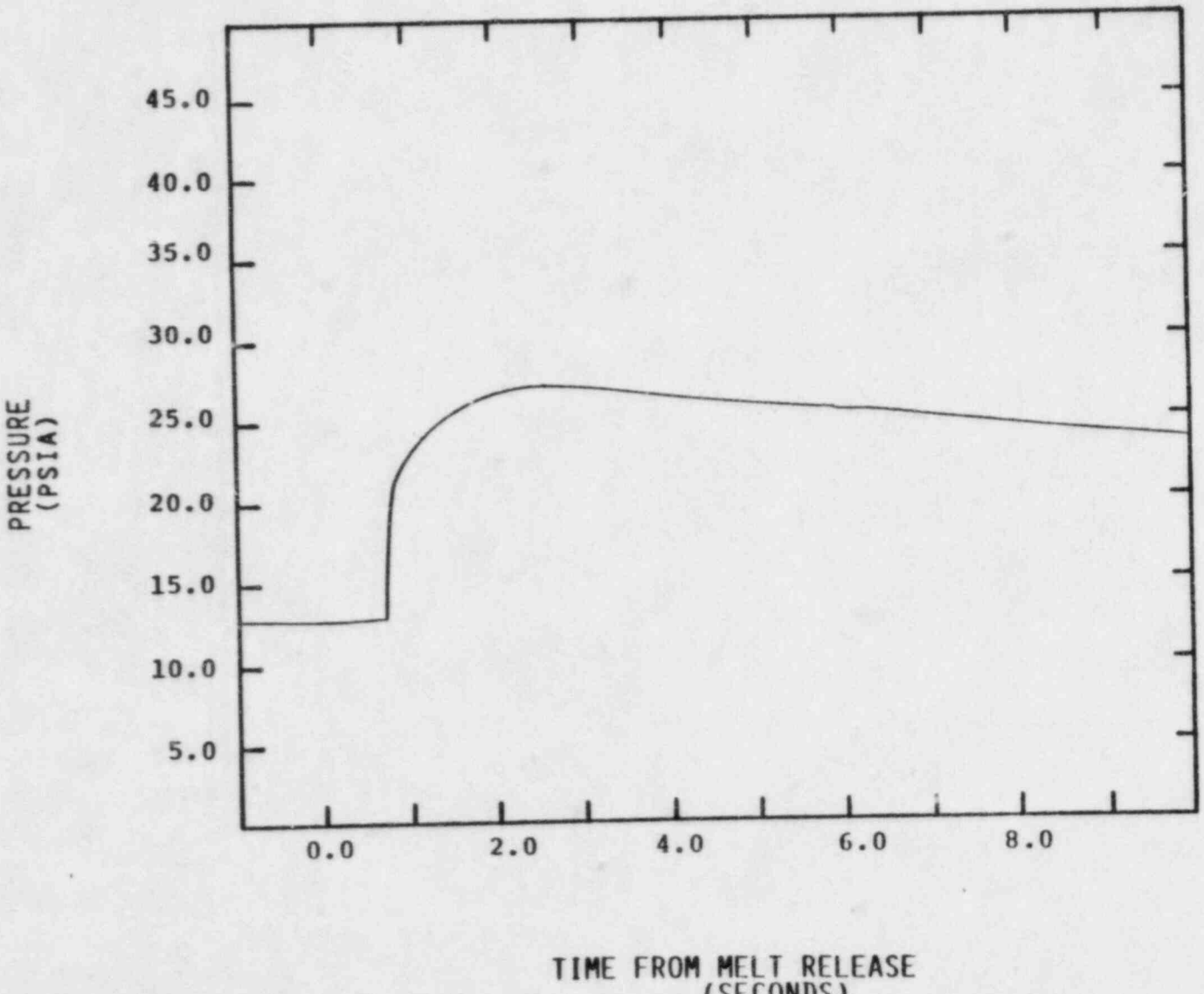

FIGURE 1. CHAMBER PRESSURE AS A FUNCTION OF TIME FOR TEST FITS 1D.

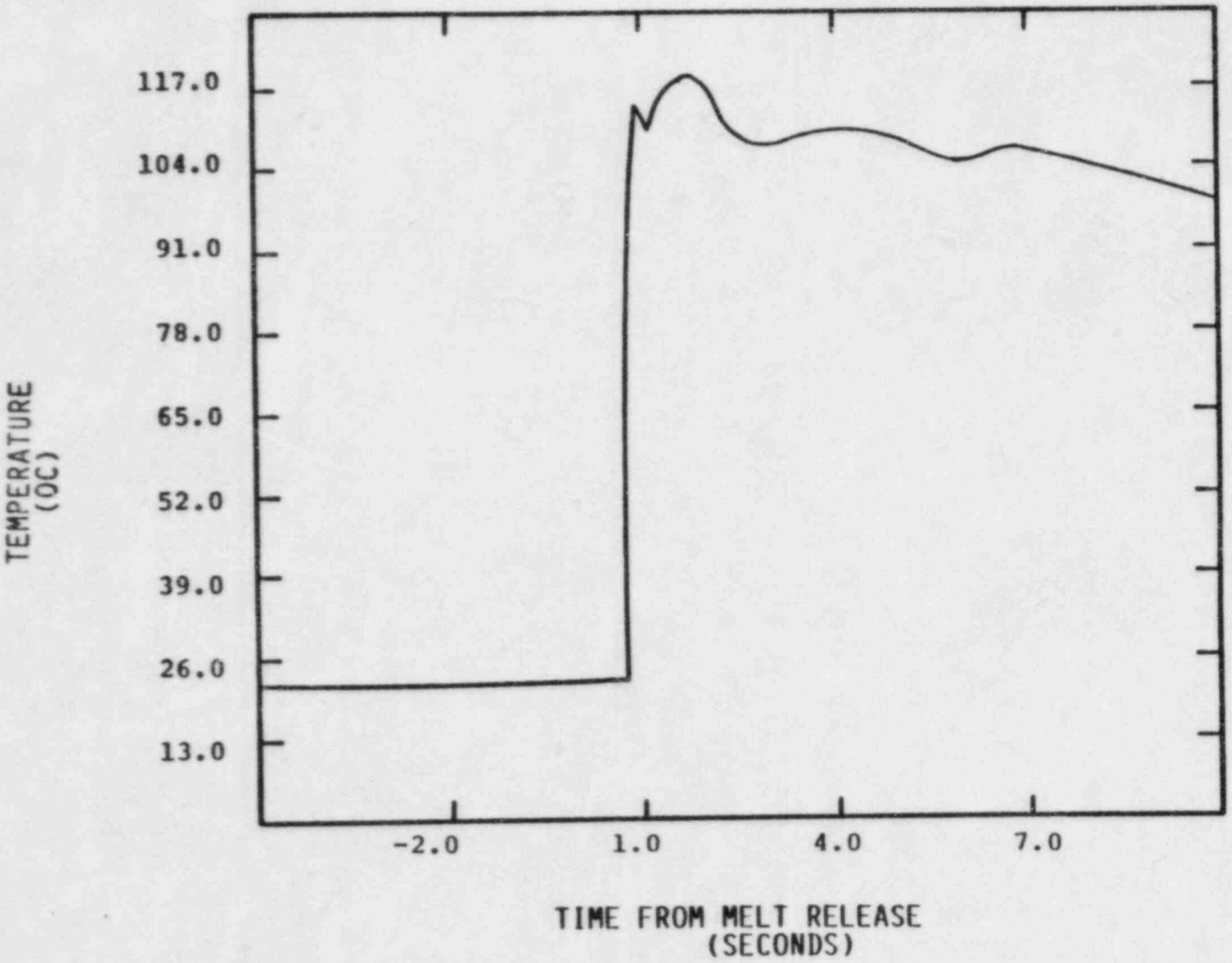

FIGURE 2. CHAMBER TEMPERATURE AS A FUNCTION OF TIME FOR TEST FITS ID.

temperature change recorded for this experiment are quite different from those for earlier explosive events.

The metal-water reaction during the course of the experiment resulted in a 20 percent by volume hydrogen content.

2.2.4 Conclusion

The nonexplosive FCI appears to produce chamber pressurization that is different in character from that produced by explosive interactions. The ultimate quasi-static level of pressurization, however, based on the 1D test, seems to be similar to that level achieved during explosive interactions. Hydrogen generation also appears similar for some of the explosive and nonexplosive events. Further investigation of the mechanisms leading to indirect containment failure are planned as soon as a revised test plan has been approved by the NRC.

3.0 Limits to Fuel-Coolant Mixing

(M. L. Corradini)

Prolonged failure of normal and emergency coolant flow in a light water reactor would cause melting of the reactor fuel, and eventual contact with residual water in-vessel or ex-vessel. This fuel-coolant contact would allow the fuel to mix with the coolant producing steam and hydrogen as the fuel slowly fragments while in film boiling. This 'premixing' phase of the fuel-coolant interaction also sets up the initial conditions for a possible steam explosion that may follow. It is our intent in this discussion to review past analysis on this 'premixing' phase of a fuel-coolant interaction (FCI), and to point out possible limits to this fuel-coolant mixing. Identification of mixing limits is of interest, because it may restrict the size of large scale steam explosions; the implication of this result would be to limit the steam explosion damage potential.

Past Work in Fuel-Coolant Mixing

Past research into fuel-coolant mixing (sometimes called 'premixing') has been directed at predicting the physical limits for which mixing could or could not occur. Fauske, et al. [1,2] originally proposed that the fuel-coolant interface temperature upon liquid-liquid contact must exceed the spontaneous nucleation temperature to allow premixing of the fuel and coolant in an energetic FCI (steam explosion). The spontaneous nucleation temperature is equal to the

homogenous nucleation temperature for a perfectly wetted system [2]. The physical picture was that stable film boiling is established above this limit for a liquid-liquid system, and this allows the fuel time to penetrate and mix within the coolant. For the LWR system, the fuel and coolant easily satisfy this criterion. It should be pointed out that this criterion is a necessary but not necessarily a sufficient criterion for 'premixing.'

Cho, et al. [3] considered the energy requirements for fuel fragmentation for both the premixing phase and the rapid fuel fragmentation phase during a steam explosion. The analysis indicated that the fuel during fragmentation must overcome surface energy, kinetic energy, and frictional dissipation to break up to smaller diameters and mix with the surrounding coolant. In situations of practical interest, Cho pointed out that the mixing energy requirements are primarily due to frictional dissipation, and other contributions may be ignored [3]. He then derived two models to estimate this mixing energy. If the fuel mass were to be mixed in one-step with the surrounding coolant, the mixing energy is given by

$$E_m|_{\text{one-step}} = \frac{3}{8} C_D \frac{\rho V_f^2}{t_m^2 R_f} \qquad (1)$$

where

V_f is the initial volume of the fuel mass to be mixed,
ρ is the average density of the surrounding fluid,
t_m is the mixing time,
C_D is the local drag coefficient, and
R_f is the final radius of the fuel after mixing has occurred.

If the fuel mass were to be mixed in a series of progressive mixing steps so as to minimize the required mixing energy, the resultant expression is

$$E_m|_{\text{min}} = 1.81\, C_D\, \rho\, V_f \left[\frac{V_f^{\frac{2}{3}}}{t_m^2}\right]\left[1 - \frac{R_f^2}{V_f^{\frac{2}{3}}}\right] \ln\left[\frac{V_f^{\frac{1}{3}}}{R_f}\right] \qquad (2)$$

One notes that the difference in these two estimates is essentially proportional to the ratio of the final fuel radius to its initial size

$$\frac{E_m|_{min}}{E_m|_{one\text{-}step}} \doteq \frac{R_f}{V_f^{\frac{1}{3}}} \ln \frac{V_f^{\frac{1}{3}}}{R_f} \qquad (3)$$

and can be large if the ratio of the final fuel radius to the initial volume is small. From this analysis, Cho made the following observations. First, the mixing energy required for fuel fragmentation must be considered in relation to the ultimate source of energy in this system, i.e., the internal energy of the fuel. For the fuel-coolant system, one requires $E_m < E_{f_o}$, where E_{f_o} is the initial fuel internal energy. Second, for a given mixing energy, Equations (1) and (2) define the maximum volume of fuel that could mix with coolant as a function of t_m and R_f. For the LWR system, the energy for premixing, E_m, is very small compared to the internal energy of the fuel, E_{f_o}.

Fauske and Henry [4,5] subsequently proposed the physical concept that for the fuel to exist in a premixed configuration with the coolant, a conceptual picture like that in Figure 1 must be achieved and sustained. If this configuration breaks down by driving the liquid water away from the molten fuel, discrete fuel particles would coalesce into larger particles and reverse the fragmentation-mixing process. Therefore, the film boiling heat flux can be equated to the capability of the water to stay mixed with fuel under the imposed steam flow. Fauske, et al. estimated this capability from the pool boiling critical heat flux. He equated the energy lost by the fuel with the maximum energy that could be removed by the steam flow (i.e., q''_{CHF}) and estimated the minimum fuel diameter during mixing, D_{min}, below which the steam flow would fluidize and drive the liquid water out of the mixture,

$$D_{min} = \frac{6\, m_f\, q''_{DROP}}{\rho_f\, A_{CHAM}\, q''_{CHF}} \qquad (4)$$

where

m_f is the fuel mass in the mixture,
A_{CHAM} is the cross-sectional area of the chamber,
ρ_f is the fuel density, and
q''_{DROP} is the heat flux from the fuel droplet given by black body radiation and film boiling heat transfer.

$$q''_{DROP} = \sigma_T(T_f^4 - T_{sat}^4) + h_{film}(T_f - T_{sat}) \qquad (5)$$

where

T_f is the fuel temperature,
T_{sat} is the coolant saturation temperature,
σ_T is the Stephan-Boltzmann constant, and
h_{film} is the film boiling heat transfer coefficient.

Fauske and Henry also pointed out that this steady state model can be used to estimate the maximum mass of fuel that could mix with the water coolant assuming some 'premixing' diameter, D_{mix}

$$m_{f_{max}} = \frac{\rho_f A_{CHAM} D_{MIX} q''_{CHF}}{6\, q''_{DROP}} \; . \qquad (6)$$

For in-vessel reactor considerations (PWR specifically), Fauske points out that no more than 100 kg of fuel could mix with the water coolant for saturated water at a pressure of one bar and D_{mix} = 10 mm. The assumption that a one-dimensional steady state CHF model is applicable under these conditions warrants further discussion.

Theofanous and Saito [6,7] also addressed the question of a limit to fuel-coolant mixing but took a different approach. Instead of investigating steady state limits to mixing, they concluded that the mixing process would be driven by the hydrodynamics of transient jet breakup as the fuel pours into a water coolant pool. Corresponding to this conceptual picture (Figure 2), they identified three regions where mixing may progressively occur: vertical jetting, horizontal jetting, vertical rise, and fallback. Surface instabilities (i.e., Rayleigh-Taylor and Kelvin-Helmholtz) in each one of these phases would produce fuel breakup and mixing. Gravitational settling due to density differences, on the other hand, would promote separation and retard mixing. The relative importance of these competing

processes would vary among the various phases and would be influenced by the diameter of the entering jet, D_j. Theofanous then quantitatively considered the effect of jet sizes from small pour streams to jet diameters approaching the size of the fuel volume. His order-of-magnitude calculations indicated that only a few percent of the available fuel mass could mix with the water coolant for in-vessel core melt situations. This represents 2500-4000 kg of fuel that could mix to characteristic mixing diameters of 10-100 mm. The major reason that more mixing could not occur was because the available time for hydrodynamic mixing was limited because the water depth in the lower plenum of the reactor vessel (PWR for these example cases) was relatively limited. For ex-vessel fuel-coolant mixing, he estimated that about 10 percent of the available molten fuel mass could mix (~13,000 kg for a PWR system).

More recently, Corradini, et al. [8,9] have attempted to analyze the Sandia fuel-coolant interaction experiments [10-12] designated as the FITS tests (FITS -- Fully Instrumented Test Series).

The fuel-coolant mixing in the FITS experiments was observed by viewing high-speed movies of the interaction. These tests involved pouring a fuel simulant (2 to 20 kg of molten Fe-Al_2O_3 at 3000 K) into a water pool (30-450 kg of water at 283 to 367 K) to simulate fuel-coolant interactions in a pouring contact mode. The conceptual picture of the fuel-coolant interaction zone was one where the fuel enters the water pool as a single discrete mass (an elongated ellipsoidal shape) in film boiling and begins to fragment. As it falls through the pool, it continues to break apart into smaller pieces and mix with the surrounding water while in film boiling. These smaller fuel particles may subdivide further as the steam produced in film boiling flows out through the top of the fuel-coolant mixture and escapes the water pool, and water flows in from the sides. The mixture grows radially as the fuel, now mixed with water and steam, spreads and falls to the chamber base (Figure 3). Two events are possible: either an energetic FCI (steam explosion) is triggered during the fall or the 'premixed' molten fuel settles on the chamber base and eventually quenches.

Corradini analyzed the observed mixing process with a characteristic dimensionless time derived from hydrodynamic considerations and was able to correlate the available mixing data so that one could find the time history of the mixing volume, the displaced water volume, and visual

observation of fuel fragment sizes. From these correlations, one could calculate the integral fuel, vapor, and liquid coolant volume fractions as functions of time. In addition, based on fluidization arguments, Corradini developed a simple steady state model that predicted the minimum fuel diameter that could exist in the mixture before the liquid fuel or coolant would be fluidized by the steam flow. In all cases of interest, coolant fluidization occurred first, so the minimum fuel diameter was given by

$$D_{min} = \left(\frac{3}{4}\right)^{\frac{1}{3}} \left[\frac{\alpha_f}{\alpha_c}\right]^{\frac{2}{9}} \left[\frac{\alpha_f}{\alpha_v}\right]^{\frac{2}{3}} \left[6\,\frac{q''_{drop}}{\rho_v i_{fg}}\right]^{\frac{2}{3}} \left[\frac{C_D H_c^2}{g}\right]^{\frac{1}{3}} \left[\frac{\rho_v}{\rho_c}\right]^{\frac{1}{3}} \tag{7}$$

where

q''_{drop} and C_D are previously defined, and

α is the volume fraction for fuel, f, vapor, v, and liquid coolant, c, respectively,

ρ is the density for fuel, f, vapor, v, and liquid coolant, c, respectively,

i_{fg} is the latent heat of vaporization,

H_c is the depth of the water pool.

To use this model, one must know the volume fraction of the fuel, vapor, and liquid coolant at a given point in time; this is obtained by using the empirically correlated values for α_f, α_v, and α_c from the FITS data [8].

In addition to this simple model for the minimum mixing diameter, Corradini and Moses [9] have developed a dynamic mixing model (WISCI) which predicts the fuel breakup as it falls through the gas atmosphere into the water pool, eventually reaching the chamber base and quenching or undergoing a steam explosion (Figure 4). The model considers the fuel to fragment due primarily to hydrodynamic forces, and the fuel diameter is taken to be

$$D_f = D_{f_o} \exp(-T^+) \tag{8}$$

where

$$T^+ \equiv \frac{v_f t}{D_{f_o}} \left[\frac{\rho_c}{\rho_f}\right]^{\frac{1}{2}} \tag{9}$$

t is time,

v_f is the fuel fall velocity, and

D_{f_o} is the initial fuel diameter.

Now, within this context of dynamic mixing, coolant fluidization, which would limit mixing, could be applied [9]. This limit in the dynamic model is a function of the fuel temperature, the water depth, since $H_c \sim v_f t$, the fuel initial size, D_{f_o}, and the mixing phenomena from the FITS tests [10,11,12] as empirically correlated [8]. If one combines these factors, one can solve for the fuel diameter after mixing as a function of H_c and D_{f_o} (see Figure 5). One can also plot the fluidization limit for different fuel temperatures assuming for the moment blackbody radiation. All the diameters to the left of the fluidization mixing limit for a given fuel temperature can mix without fluidization, while those diameters to the right of the limit for a given H_c and D_{f_o} will begin to fluidize. This dynamic model for mixing and mixing limit only considers the leading edge (i.e., an equivalent spherical volume) of the entering fuel jet to be capable of mixing. The fuel mass behind this leading edge can also mix but must first undergo jet breakup into discrete fuel masses based upon mechanisms as outlined by Theofanous in his discussions [6,7].

Applicability of Mixing Limits

If one compares the work of the previous investigators, one notes that mixing energy requirements do not limit the amount of fuel that can mix with the coolant; rather, it is hydrodynamic considerations either due to boiling processes [4,5], or transient jet breakup [6,7], or some combination of these two effects [8,9] that limit mixing. The second observation one can make is that for a given set of conditions (e.g., one atmosphere, saturated water, PWR geometry neglecting structure), these fuel-coolant mixing limits yield a range of results (see Tables 1 and 2). One notices that the results of Theofanous and Corradini are similar even though the specific analyses are different.

The prediction using the model of Fauske is substantially lower in both the in-vessel and ex-vessel cases. The reason for the differences seem to be due to the use of the pool boiling critical heat flux as a measure of the limit of mixing due to coolant fluidization. In the model, the energy released from the fuel by heat transfer is equated to the maximum energy that can be removed from the mixture, and the maximum mass mixed given $D_{f_{mix}}$ is then calculated

$$\frac{6m_f}{\rho_f D_{f_{mix}}} q''_{DROP} = A_{CHAM}\, q''_{CHF} \tag{10}$$

where the terms have been previously defined, and where the maximum energy that can be removed is taken to be the cross-sectional area times the pool boiling critical heat flux. Now this model assumes the fuel-coolant mixture is in steady state and occupies the whole chamber cross-sectional area (Figure 1) down to the chamber base, and that the only way water coolant can enter the mixture region is from above counterflow to the steam that is being produced and must leave the mixture. (One should remember that both Theofanous and Corradini have noted the multidimensional nature of the real fuel-coolant mixing process.) The limit to mixing then corresponds to the point when the water flowing downward is fluidized by the steam upflow. One could recast the model in these terms to be

$$\frac{6m_f}{\rho_f D_{mix}} q''_{DROP} = \rho_v\, i_{fg}\, A_{CHAM}\, v_{SC_{CHF}} \tag{11}$$

where the energy removed per unit volume is $\rho_v i_{fg}$ and $v_{SC_{CHF}}$ is the critical superficial steam velocity that will fluidize the water coolant.

Now, if one takes Kutateladze's or Zuber's model [13] for the critical heat flux in pool boiling as Fauske used, one finds that $v_{SC_{CHF}}$ is given by

$$v_{SC_{CHF}} = 0.14 \left[\frac{\sigma g(\rho_c - \rho_v)}{\rho_v^2}\right]^{\frac{1}{4}} \tag{12}$$

where the constant 0.14 was determined empirically from pool boiling data. Later, Borishanskii [14] indicated that this empirical constant can be explained in terms of the hydrodynamic size of the liquid and vapor as the critical heat flux is reached and their relative viscosities. The functional form of the characteristic velocity given in Equation (12) can be easily explained in terms of liquid coolant fluidization assuming that the coolant is conceptually considered to be droplets with a diameter derived from hydrodynamic stability.

Assume Fauske's concept for a steady state limit is valid for the moment. Let us derive a mixing limit based on coolant fluidization and compare it to the CHF model. Consider a coolant droplet with a diameter, D_c; if this droplet were to become fluidized by the surrounding vapor flow, a simple force balance gives us this fluidization velocity, v_{fl}

$$v_{fl} = \left[\frac{4}{3} g \frac{D_c}{C_D} \frac{(\rho_c - \rho_v)}{\rho_v}\right]^{\frac{1}{2}} \tag{13}$$

where all the terms have been previously defined. Now, for a collection of coolant droplets, the local vapor velocity would increase due to the volume occupied by the coolant and the local drag coefficient would also increase due to this same effect. Using the empirical results from Wallis [15] on the drag coefficient in an array of particles, the superficial critical fluidization velocity becomes

$$v_{sc} = \alpha_v \left[\frac{4}{3} g \frac{D_c}{C_D(\alpha_c)} \frac{(\rho_c - \rho_v)}{\rho_v}\right]^{\frac{1}{2}} \tag{14}$$

where

$$C_D(\alpha_c) = \frac{C_{D_s}}{(1 - \alpha_c)^{4.65}} \tag{15}$$

where C_{D_s} is the drag coefficient for a single sphere.

The next question to consider is what is the proper value for the coolant characteristic length scale, D_c. In the real case for the fuel-coolant mixture in the FITS experiments [10-12], the coolant liquid and vapor occupy essentially equal volumes with the fuel having a relatively low volume fraction ($\alpha_v \sim 0.49$, $\alpha_c \sim 0.49$, $\alpha_f \sim 0.02$). The coolant liquid is actually the continuous phase in this case, so one characteristic length is to consider the coolant liquid between individual fuel droplets

$$D_{c_1} = D_f \left[\frac{\alpha_c}{\alpha_f}\right]^{\frac{1}{3}} \quad . \tag{16}$$

If one substitutes this value into Equation (14), one gets

$$v_{sc_1} = \alpha_v \left[\frac{4}{3} g \frac{D_f \left[\frac{\alpha_c}{\alpha_f}\right]^{\frac{1}{3}}}{C_D(\alpha_c)} \frac{\Delta\rho}{\rho_v}\right]^{\frac{1}{2}} \quad . \tag{17}$$

Comparing this superficial fluidization velocity to that given in the CHF model (Equation (12)), one notes that this model results in larger velocities to initiate fluidization; for conditions similar to those in Table 1, the ratio of v_{sc_1} to $v_{sc_{CHF}}$ is 14 to 1 for an assumed mixing diameter, $D_{f_{mix}} = 100$ mm.

Now, the coolant length scale used previously neglects the fact that if the coolant liquid begins to fluidize, it will begin to break up and fragment to sizes given by the critical Weber number for the coolant

$$D_{c_2} = \frac{We_{crit}\sigma}{\rho_v v_{sc}^2} \tag{18}$$

where σ is the surface tension. If one substitutes this length scale into Equation (14), one gets

$$v_{SC_2} = \alpha_v \left[\frac{4}{3} \frac{We_{crit}}{C_D(\alpha_c)} \frac{g\sigma\Delta\rho}{\rho_v^2} \right]^{\frac{1}{4}} \quad (19)$$

Comparing this fluidization velocity to that from the CHF model (Equation (12)), once again this model results in larger velocities; for conditions similar to those in Table 1, the ratio of v_{SC_2} to $v_{SC_{CHF}}$ is 4.4 to 1.

The actual coolant length scale would be between these two bounds because the actual fuel-coolant mixing process is probably a transient phenomena. This can be demonstrated by considering the time it takes the coolant with a characteristic length given by Equation (16) to break apart due to steam flow down to the characteristic length given by Eq. (18). This is a classic case of hydrodynamic breakup where the time for breakup is given by

$$T^+ = 3 \text{ to } 6 \quad (20)$$

where as before, T^+ is defined as

$$T^+ \equiv \frac{v_{SC_2} t_B}{D_{c_1}} \left[\frac{\rho_v}{\rho_c} \right]^{\frac{1}{2}} \quad (21)$$

For our example case assuming $T^+ = 4$, one finds the time for breakup, t_B, is on the order of a few seconds. A few seconds are greater than or equal to the time it takes the fuel to pour into the coolant pool both for in- and ex-vessel situations.

This result is quite representative of many initial conditions and indicates that the mixing process even considering one-dimensional counter-flow coolant fluidization may not be a steady state process, but inherently transient; i.e., even the coolant length scale that could fluidize would change with time. Therefore, if one were to use the Fauske model, its derivation from first principles (as done here) would result in a range of fuel masses that could mix, rather than one single mass. Also, this range of fuel masses that could premix agrees with the results of Theofanous and Corradini quite well, where similar values for the assumed mixing diameter, $D_{f_{mix}}$, are used (see Figure 6).

Current Conclusions

A number of models have been advanced that attempt to predict the limit to mixing for molten fuel pouring into a water coolant during the 'premixing' phase of an FCI. These models are all first order estimates and are based on the concept that hydrodynamic considerations limit how much fuel can mix with the coolant due to transient jet breakup phenomena and coolant fluidization limits. A wide range in the prediction of how much fuel could mix with the coolant under certain reactor in-vessel or ex-vessel situations was originally noted. Upon investigation of the Fauske model based on critical heat flux and a simple first principles derivations of it for coolant fluidization, it was found that the derived mixing limit is actually in reasonable agreement with the other models when uncertainties are included. The concept of a steady-state fuel-coolant mixing limit may be inherently flawed, because the coolant as it is being fluidized and the fuel as it enters the pool is undergoing transient breakup. Theofanous pointed this out quite clearly for the fuel in his mixing limits, because his model primarily dealt with transient fuel jet breakup. A simple calculation of the range of characteristic coolant diameters for fluidization and the time to go from an initial size to a final stable size also indicates the transient aspects of this mixing phenomenon.

Finally, one should point out that fuel-coolant mixing is inherently a multidimensional process, and current models have indicated some aspects of how this should be considered. In future work, it is recommended that the transient and multidimensional aspects of the fuel-coolant mixing phenomena be more actively investigated.

References

1. Fauske, H. K., "Some Aspects of Liquid-Liquid Heat Transfer and Explosive Boiling," Proc. Fast React. Safety Mtg., Beverly Hills, CA, (1974).

2. Henry, R. E., and Fauske, H. K., "Nucleation Characteristics in Physical Explosions," Proc. of Third Spec. Mtg. on Sodium-Fuel Inter. in Fast React., Tokyo, Japan, (1976).

3. Cho, E. H., et al., "Mixing Considerations for Large-Mass Energetic Fuel-Coolant Interactions," Proc. ANS/ENS Fast React. Safety Mtg., Chicago, IL, CONF-761001, (1976).

4. Henry, R. E. and Fauske, H. K., "Core Melt Progression and the Attainment of a Permanently Coolable State," Proc. of Thermal React. Fuels Mtg., Sun Valley, ID, (1981).

5. Henry, R. E. and Fauske, H. K., "Required Initial Conditions for Energetic Steam Explosions," Fuel-Coolant Interactions, ASME HTD-V19, Washington, DC, (1981).

6. Meyer, J. F., et al., Preliminary Assessment of Core-Melt Accidents at the Zion and Indian Point Nuclear Power Plants and Strategies for Mitigating Their Effects, Appendix B, NUREG-0850, Vol. 1, U.S. Nuclear Regulatory Commission Report (1981).

7. Theofanous, T. G. and Saito, M., "An Assessment of Class-9 (Core-Melt) Accidents for PWR Dry-Containment Systems," Purdue University Report, PNE-81-148, (Jan., 1981).

8. Corradini, M. L., "Proposed Model for Fuel-Coolant Mixing During a Core Melt Accident," Proc. Int'l. Mtg. on Thermal Reactor Safety, NUREG/EC-0027 (August 1982).

9. Corradini, M. L. and Moses, G. A., "A Dynamic Model for Fuel-Coolant Mixing," Proc. Int'l. ANS/ENS Meeting on Severe Accident Evaluation, Cambridge, MA (August 1983).

10. Berman, M., LWR Safety Quarterly, Sandia National Laboratories, SAND80-1304, Jan.-March, April-June, July-Sept., Oct.-Dec. (1980); SAND81-1216, Jan.-March, (1981); SAND82-0006, April-Sept. (1981); SAND82-1572, Oct. 1981-March 1982 (1982); April-Sept. 1982; SAND 83-1576 (1983).

11. Mitchell, D. E., et al., Intermediate Scale Steam Explosion Phenomena: Experiments and Analysis, SAND81-0124, NUREG/CR-1245, Sandia National Laboratories (September 1981).

12. Mitchell, D. E. and Evans, N. A., "The Effect of Water to Fuel Mass Ratio and Geometry on the Behavior of Molten Core-Coolant Interaction at Intermediate Scale," Proc. Int'l. Mtg. on Thermal Reactor Safety, NUREG/CP-0027 (August 1982).

13. Zuber, N., "On the Stability of Boiling Heat Transfer," Transactions of the ASME, 711-720 (April 1958).

14. Borishanskii, Z. M., "An Equation Generalizing Experimental Data on the Cessation of Bubble Boiling in a Large Volume of Liquid," Zhurn. Tekh. Fiz., V26, p. 452 (1956), translated in Soviet Physics-Technical Physics, VI, p. 438 (1957).

15. Wallis, G., One-Dimensional Two-Phase Flow, McGraw-Hill, New York, (1981).

Table 1

In-Vessel Fuel-Coolant Mixing Limits*

	Mixed Mass (M_{max}-kg)	Fuel Diameter (D_{mix}-mm)
Fauske, et al. [4,5]	100	10
Theofanous [6,7]	2500-4000	10-100
Corradini, et al. [8,9]	3000-5000	60-100

*·PWR geometry in-vessel water depth 3 m

vessel cross-section 15 m^2

structure in lower plenem is neglected

·Pressure - 1 atmosphere

·Saturated water

·Fuel temperature - 2700 K; with black-body radiation

Table 2

Ex-Vessel Fuel-Coolant Mixing Limits*

	Mixed Mass (M_{max}-kg)	Fuel Diameter (D_{mix}-mm)
Fauske, et al. [4,5]	200	10
Theofanous [6,7]	13000	10-100
Corradini, et al. [8,9]	13000-16000	75-100

*·PWR geometry ex-vessel water depth in cavity 5 m

cavity cross-sectional area 30 m^2

structure in cavity is neglected

·Pressure - 1 atmosphere

·Saturated water

·Fuel temperature - 2700 K; with black-body radiation

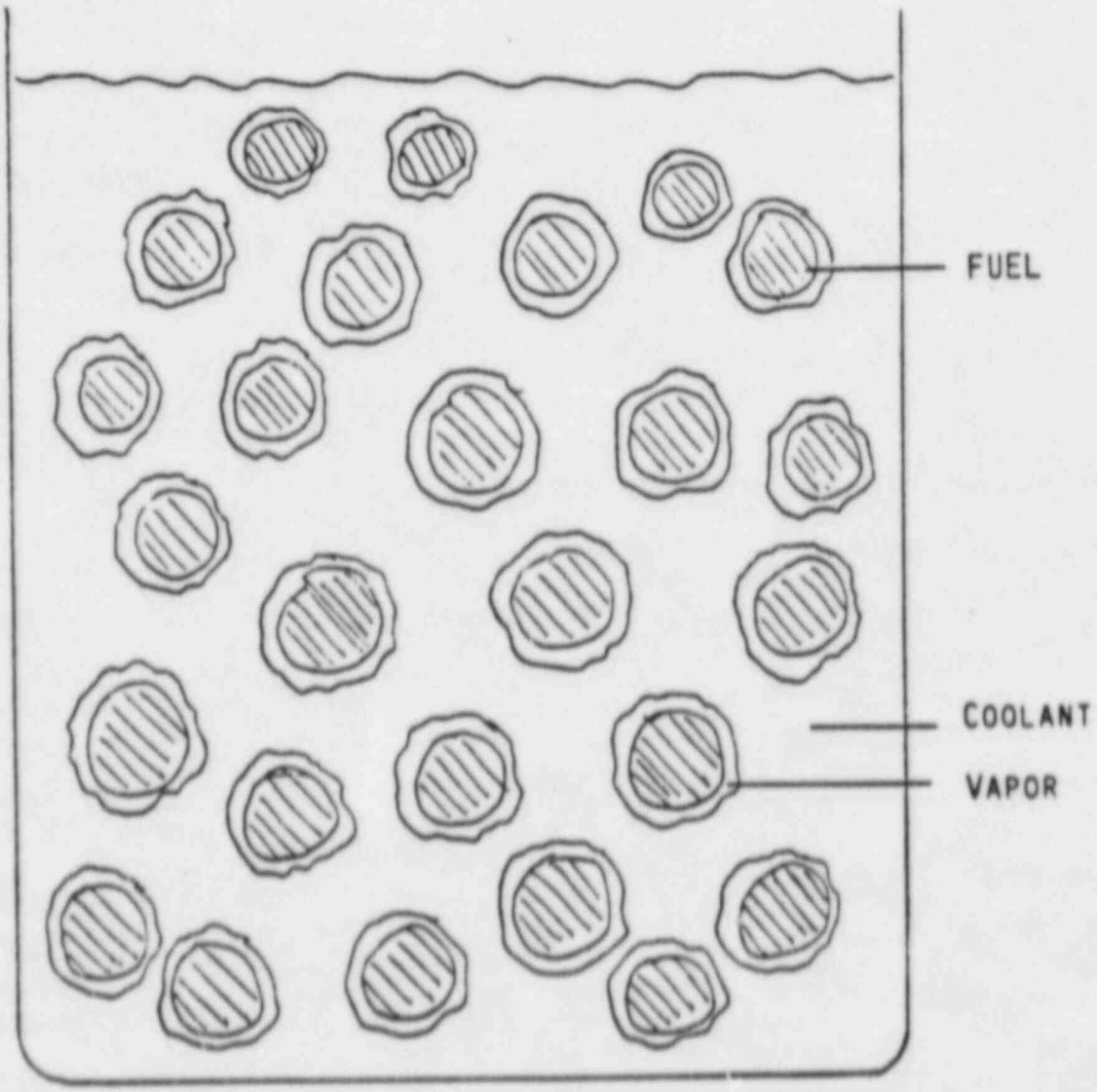

Figure 1

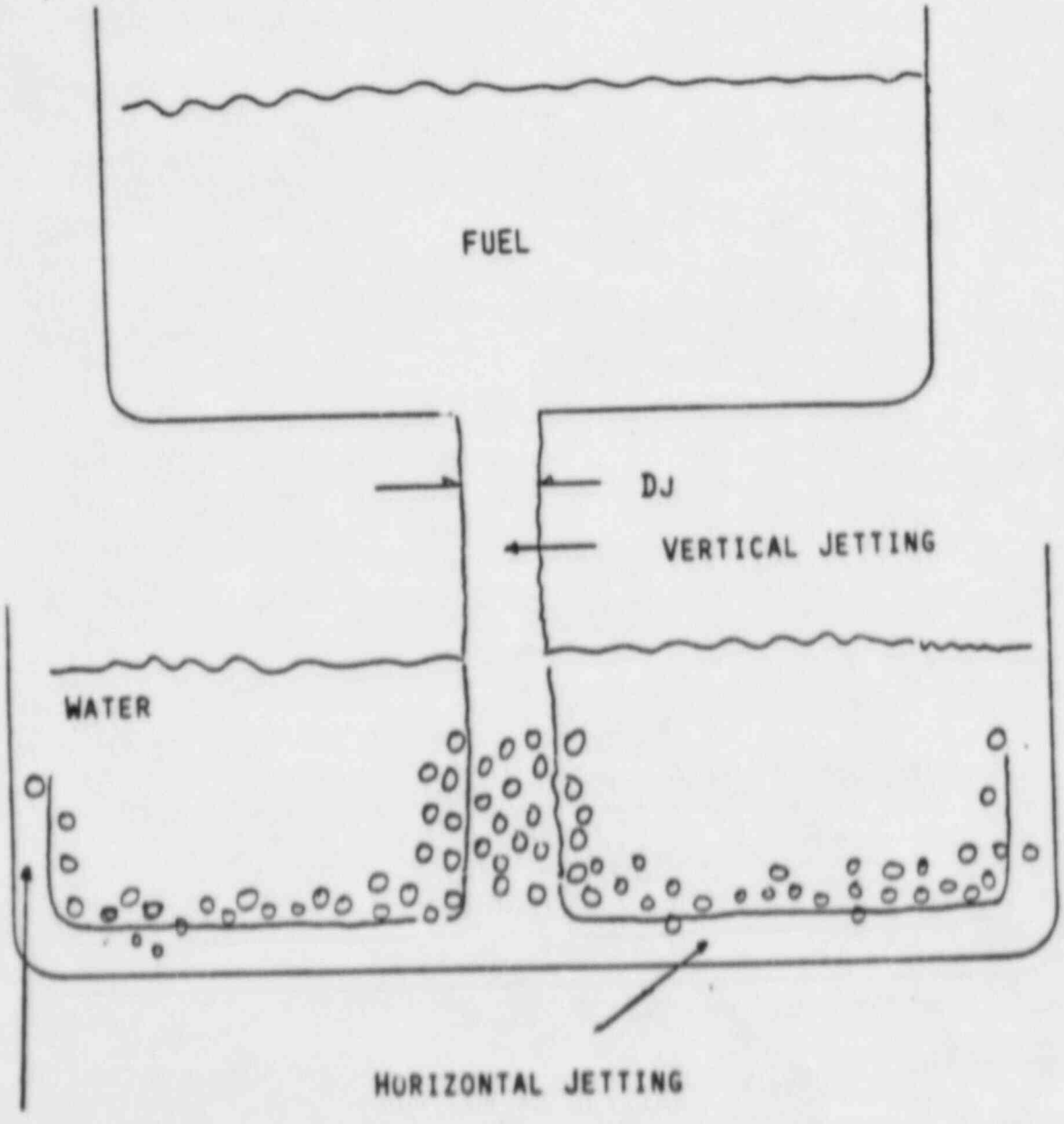
FUEL
DJ
VERTICAL JETTING
WATER
HORIZONTAL JETTING
VERTICAL RISE
AND FALLBACK

Figure 2

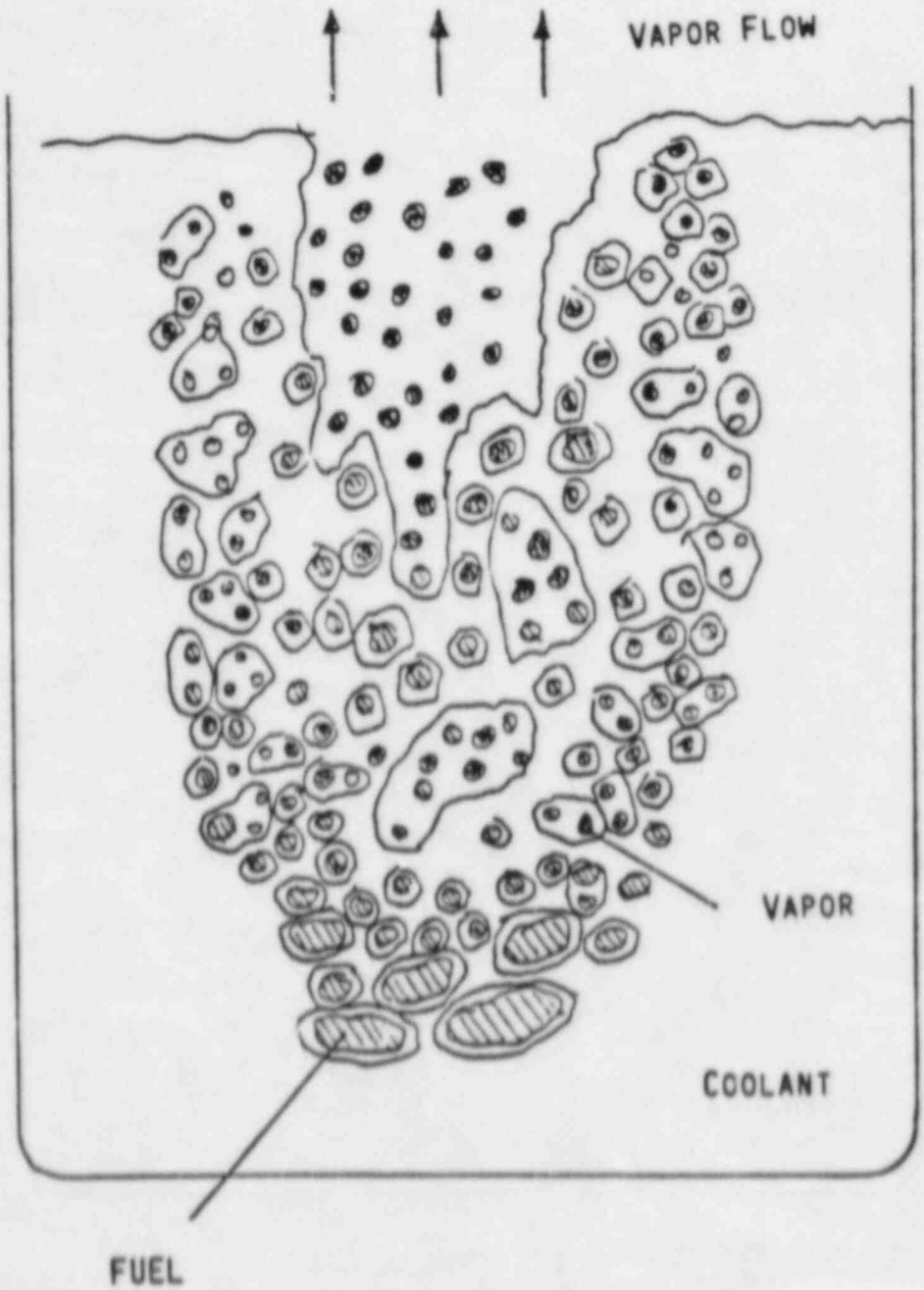

Figure 3

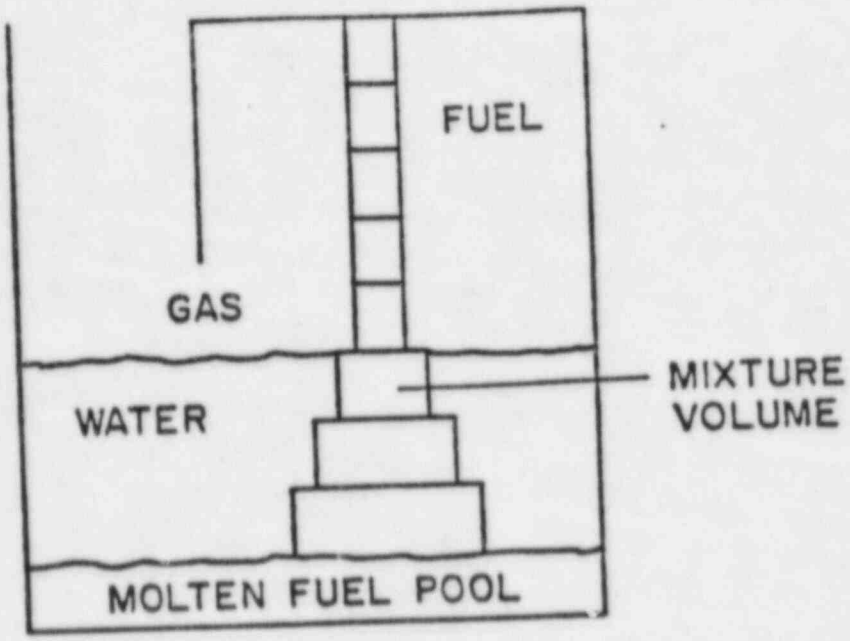
FUEL
GAS
WATER
MIXTURE
VOLUME
MOLTEN FUEL POOL

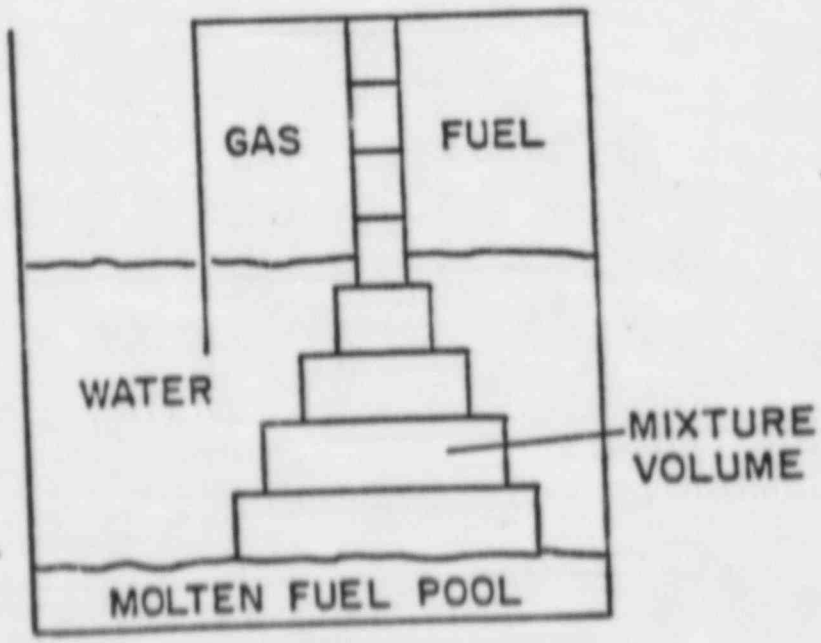
GAS
FUEL
WATER
MIXTURE
VOLUME
MOLTEN FUEL POOL

Figure 4

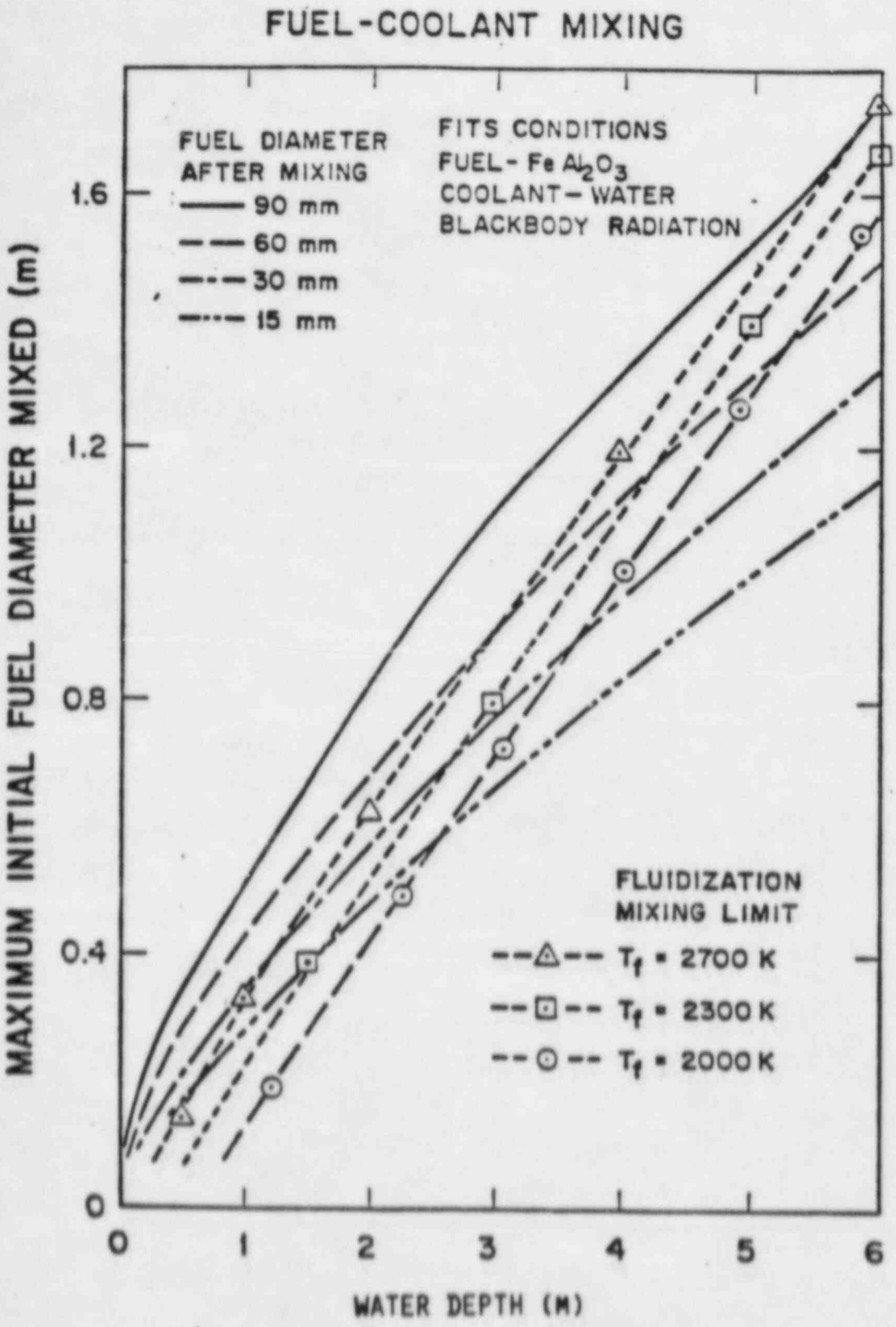
FUEL-COOLANT MIXING
FUEL DIAMETER AFTER MIXING
90 mm
60 mm
30 mm
15 mm
FITS CONDITIONS
FUEL - Fe Al2O3
COOLANT - WATER
BLACKBODY RADIATION
FLUIDIZATION MIXING LIMIT
Tf = 2700 K
Tf = 2300 K
Tf = 2000 K
MAXIMUM INITIAL FUEL DIAMETER MIXED (m)
WATER DEPTH (M)
0
0.4
0.8
1.2
1.6
0
1
2
3
4
5
6

Figure 5

Figure 6

LIMITS TO FUEL - COOLANT MIXING

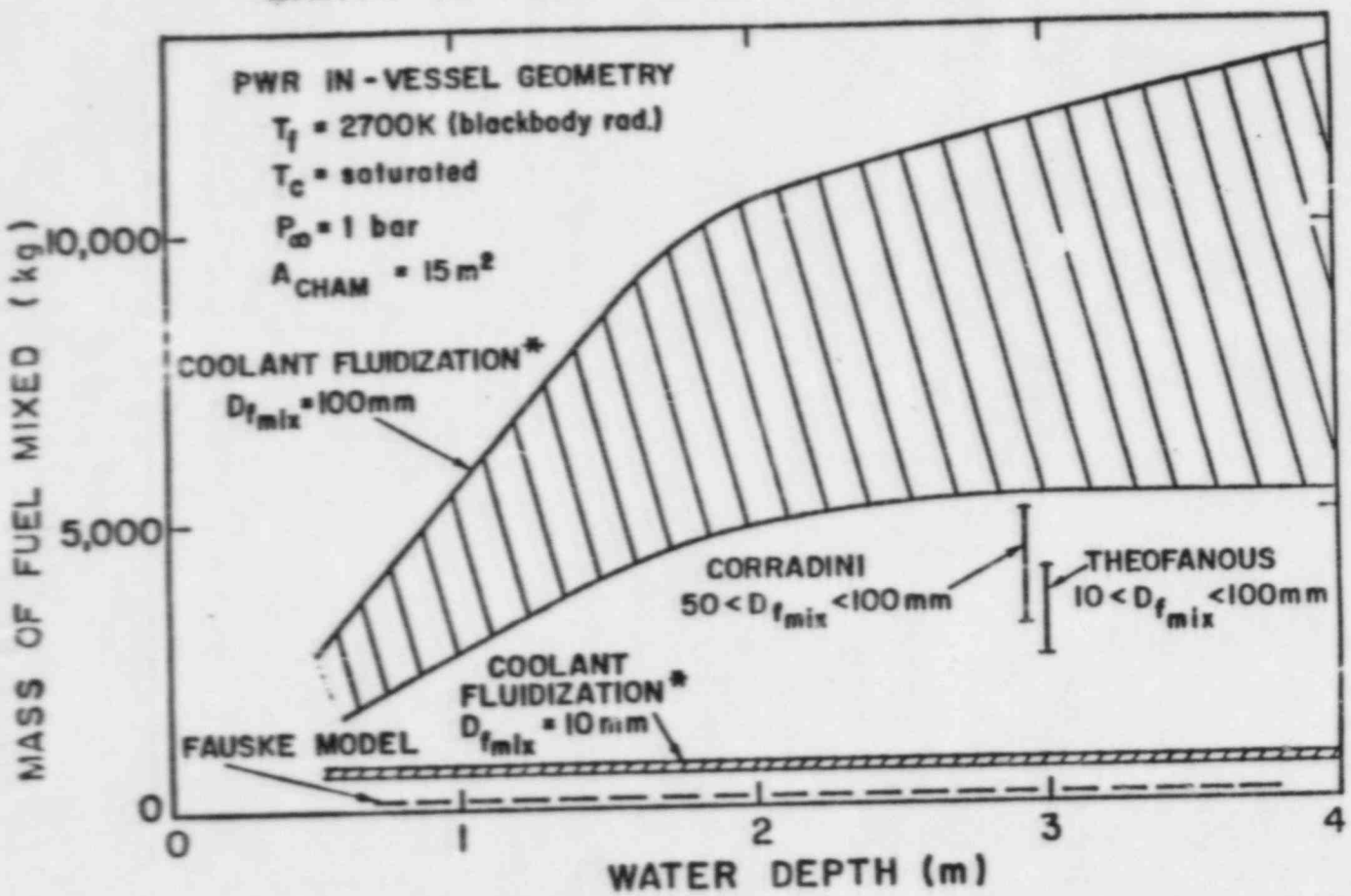

*THE RANGE OF VALUES DESIGNATED BY THE SHADED AREA IS DUE TO TWO DIFFERENT COOLANT CHARACTERISTIC DIAMETERS; ONE RELATED TO THE FUEL DIAMETER (HIGHER VALUE) AND ONE RELATED TO THE CRITICAL WEBER NUMBER DIAMETER (LOWER VALUE).

II. Molten Core/Concrete Interactions (R. K. Cole, Jr., D. P. Kelly, M. A. Ellis)

1. Presentations

CORCON calculations for a set of BWR MKI and MKII standard problems were presented to a meeting of the Containment Loads Working Group at Argonne on November 17. These calculations were performed with the latest evolutionary version of CORCON, Version 1.02.02. At the meeting, comparisons were made with CORCON-MOD1 Calculations performed by George Greene (BNL) and INTER calculations performed by various people.

In all cases, the initial melt contained substantial amounts of unoxidized zirconium, and CORCON predicted coking. That is, for as long as metallic zirconium was present, the CO_2 which passed through the pool was converted to elemental carbon and retained in the pool. When the zirconium was depleted, this retained carbon was rapidly oxidized producing a burst of CO. This was true for both 1.02.02 and MOD1; INTER chemistry does not include coking. In addition, it was observed that INTER predicted substantially more total gas generation and concrete erosion than CORCON, particularly for basaltic concrete. The effect was so great that the question was raised as to whether INTER conserved energy. One conclusion of the meeting was that the community would like CORCON-MOD2 to be released as soon as possible.

During the reporting period, we reviewed IDCOR Technical Report 15.3, "Core-Concrete Interactions," and presented our conclusions at a meeting in Harpers Ferry, WV. The IDCOR modelling is extremely simple -- almost simplistic -- compared to CORCON. While we found several areas of disagreement concerning specific models, we concluded that no firm conclusions could be reached concerning adequacy of their model until applications could be examined.

2. CORCON Development

As described in our last letter, the initial implementation of the coolant model evaluated heat transfer using an approximate boiling curve for atmospheric pressure. During this reporting period, we extended the model to include the effects of ambient pressure. This was done as follows:

The standard correlations, Zuber-Rohsenow nucleate boiling, Berenson film boiling, and the Ivey correction for subcooled nucleate boiling were used, outside of CORCON, to calculate the CHF and minimum film-boiling points (both heat flux and excess temperature) as functions of ambient pressure.

These calculations employed full temperature- and pressure-dependent water properties which, in some cases, required an iterative calculation.

The resulting data were then fit as functions of pressure alone, using simple forms which were found to agree with the detailed calculations with maximum deviations of two to three percent over the range of 0.1-100.0 bars.

Because this accuracy is quite sufficient for CORCON, these fits were incorporated into the code rather than the original correlations. The advantages are a significant savings in code complexity and a reduction in the volume of materials-property data which must be included.

We also spent a significant amount of time investigating an apparent error in the treatment of phase changes in the thermal equation-of-state package. This was ultimately traced to an error in the CDC FTN5(OPT=0) compiler. The time spent should perhaps be charged to code assessment: we are now quite sure that the coding is correct!

3. Above-Pool Modelling

A series of scoping calculations were performed using the above-pool model briefly described in the previous bimonthly report. The purpose of these calculations was to get an estimate of the contribution to overall gas generation from the ablation of above-pool structures. This calculation was performed using the latest version of the code designated as 1.02.04, which closely resembles what will soon be MOD 2. The input data were that for the sample problem (large dry PWR) given in the MOD 1 user's manual. The results are summarized below.

	Gas Generation	
	Species	Mass (kg)
Pool:	CO_2	14886.
	CO	9793.
	H_2O	3391.
	H_2	372.
Above-Pool:	CO_2	2653.
	H_2O	1378.

The inclusion of above-pool generated gases constitutes increases of approximately 41 percent and 18 percent for cumulative production of H_2O and CO_2, respectively.

4. Transient Concrete Response

In order to determine the extent to which water migration influences transient conduction in concrete, a set of calculations was performed by Ahti Suo-Anttila of org. 6425 using SLAM (Sodium Limestone Ablation Model). This program contains a detailed, finite-difference conduction with ablation model including the effect of water migration. The program has the flexibility to either include or neglect the water migration terms. Heat flux boundary conditions commonly observed in the CORCON code were simulated in SLAM for cases with and without water migration. The difference in average recession rates and gas generation for the two cases was surprisingly small, certainly less than the error due to the uncertainty associated with the thermophysical properties of concrete. We conclude from these results that water migration does not have a significant impact on concrete ablation modelling.

5. Code Assessment

During this reporting period the final writing and editing of the assessment report was completed. The internal review process has been completed, leaving only line-management approval before it can be published.

Copy to:
M. L. Corradini, U. Of Wisc.
M. Cunningham, NRC, RES
R. T. Curtis, NRC, RES
R. Denning, BCL
G. A. Greene, BNL
C. N. Kelber, NRC, RES
J. T. Larkins, NRC, RES
G. Quittschreiber, NRC, ACRS
D. F. Ross, NRC, RES
Z. R. Rosztoczy, NRC, NRR
M. Silberberg, NRC, RES
T. P. Speis, NRC, RES
D. Squarer, EPRI
R. C. Vogel, EPRI
D. Swanson
T. G. Theofanous, Purdue
R. W. Wright, NRC, RES
6400 A. W. Snyder
6420 J. V. Walker
6422 D. A. Powers
6424 K. D. Bergeron
6425 W. J. Camp
6425 W. Frid
6425 K. Schoenfeld
6425 A. J. Wickett
6425 M. F. Young
6440 D. A. Dahlgren
6427 D. P. Kelly
6427 M. S. Krein
6427 B. W. Marshall, Jr.
6427 L. S. Nelson
6427 O. Seebold
6444 J. M. McGlaun
6444 S. L. Thompson
6427 M. Berman (3)
6444 R. K. Cole, Jr.